ESAIM: PROCEEDINGS, October 2011, Vol. 32, p. 163-176
E. Cancès, N. Crouseilles, H. Guillard, B. Nkonga, and E. Sonnendrücker, Editors

FINITE VOLUME METHOD IN CURVILINEAR COORDINATES FOR HYPERBOLIC CONSERVATION LAWS *

A. Bonnement[1], T. Fajraoui[2], H. Guillard[3], M. Martin[4], A. Mouton[5], B. Nkonga[6] and A. Sangam[7]

Abstract. This paper deals with the design of finite volume approximation of hyperbolic conservation laws in curvilinear coordinates. Such coordinates are encountered naturally in many problems as for instance in the analysis of a large number of models coming from magnetic confinement fusion in tokamaks. In this paper we derive a new finite volume method for hyperbolic conservation laws in curvilinear coordinates. The method is first described in a general setting and then is illustrated in 2D polar coordinates. Numerical experiments show its advantages with respect to the use of Cartesian coordinates.

1. Introduction

We are concerned with the construction of finite volume methods in curvilinear coordinates for hyperbolic conservation laws. Such schemes are crucial when one is interested in capturing accurately the properties of the physical model under consideration in which coordinates system play an important role. The physical models of interest are for instance those describing charged particles motion in solar winds in the frame of astrophysical plasmas [4] or the transport of charged particles in a tokamak, a Magnetic Fusion Confinement device dedicated to the ignition of controlled thermonuclear fusion reactions on earth [4, 8, 10].

More precisely, in magnetized plasma, there are two distinct behaviours of particles, along and accross magnetic field lines. This leads to highly anisotropic flows of the plasma. As a consequence, Cartesian coordinates do not constitute an appropriate system to describe the physics that takes place in the plasma. Instead, other systems of coordinates are preferred, as for instance field aligned coordinates systems [1, 2], Boozer coordinates or Hamada coordinates [6]. The field governing equations written in these generalized curvilinear systems are generally not in strict conservation laws form: spatially varying metric coefficients multiply the differential terms and additional source terms appear in the equations. Therefore the design of a finite volume method is not as straighforward as it is in Cartesian coordinates and additionally important conservation properties can be lost by the discretisation. Another relevant question that arises in this context concerns the representation

* *A. Bonnement was supported in part by the Conseil Régional Provence-Alpes-Côte d'Azur.*

[1] INRIA Sophia-Antipolis & Université Nice Sophia-Antipolis, UMR CNRS 6621 (France), e-mail : audrey.bonnement@unice.fr
[2] Université Valenciennes, FR CNRS 2956 (France), e-mail : tarek.fajraoui@univ-valenciennes.fr
[3] INRIA Sophia-Antipolis & Université Nice Sophia-Antipolis, UMR CNRS 6621 (France), e-mail : Herve.Guillard@inria.fr
[4] Université Nice Sophia-Antipolis, UMR CNRS 6621 & INRIA Sophia-Antipolis (France), e-mail : marie.martin@unice.fr
[5] Université Toulouse 3, UMR CNRS 5219 (France), e-mail : alexandre.mouton@math.univ-toulouse.fr
[6] Université Nice Sophia-Antipolis, UMR CNRS 6621 & INRIA Sophia-Antipolis (France), e-mail : boniface.nkonga@unice.fr
[7] Université Nice Sophia-Antipolis, UMR CNRS 6621 & INRIA Sophia-Antipolis (France), e-mail : afeintou.sangam@unice.fr

of vectors and the choice of the basis in which these vectors are expressed since in curvilinear coordinates, the basis are spatially dependent. For instance, the projection of a vector in the local basis of the corresponding coordinates system introduces source terms coming from the variations of local basis with respect to the variables of the chosen curvilinear coordinates, and the conservation laws form of the equation is therefore lost. From a numerical point of view, finding an appropriate approximation of this kind of terms that keeps the conservation properties of the system of equations remains a challenge, for this purpose it is useful to think about source terms in shallow water systems, or to Coriolis force term in geophysical equations [7].

Our approach consists in constructing the finite volume approximation of the considered equations in general curvilinear coordinates, without any preliminar projection when dealing with vector equations. Averaged quantities are carefully chosen so that the constructed finite volume scheme is capable of capturing the principal characterics of the physical models. This approach allows to automatically approximate the non-conservative terms in a consistent manner independently of the curvilinear system used.

This paper is organized as follows. In section 2, prerequisites on curvilinear coordinates are recalled. Finite volume methods in these curvilinear coordinates are designed in section 3. Numerical tests using two-dimensional cylindrical coordinates as example are then considered in section 4 in order to illustrate our approach. Finally, conclusion is given in section 5.

2. Geometrical tools

Let us consider a physical model defined on a physical domain $\Omega(\boldsymbol{x}) \subset \mathbb{R}^3$, where each point $M(\boldsymbol{x})$ of $\Omega(\boldsymbol{x})$ is localized by its Cartesian coordinates $\boldsymbol{x} = {}^t(x^1, x^2, x^3)$. Suppose now the physical model under consideration can be easily described in another coordinates systems, so that the physical model can be looked through the domain $\Omega(\boldsymbol{\xi})$, where $\boldsymbol{\xi} = {}^t(\xi^1, \xi^2, \xi^3)$. The domain $\Omega(\boldsymbol{\xi})$ will be referred to as the computational domain, and the corresponding coordinates system $\boldsymbol{\xi}$ as curvilinear coordinates. Obviously, there exists an one-to-one map $\phi : \boldsymbol{\xi} \mapsto \boldsymbol{x}$, which is assumed to be at least a $\mathcal{C}^1$-diffeomorphism, which means that J the determinant of the Jacobian matrix M_J of ϕ defined by

$$M_J = \begin{bmatrix} \frac{\partial x^1}{\partial \xi^1} & \frac{\partial x^1}{\partial \xi^2} & \frac{\partial x^1}{\partial \xi^3} \\ \frac{\partial x^2}{\partial \xi^1} & \frac{\partial x^2}{\partial \xi^2} & \frac{\partial x^2}{\partial \xi^3} \\ \frac{\partial x^3}{\partial \xi^1} & \frac{\partial x^3}{\partial \xi^2} & \frac{\partial x^3}{\partial \xi^3} \end{bmatrix}$$

is positive. To introduce the compact expressions of the gradient and the divergence operators, $\boldsymbol{\nabla}$, $\boldsymbol{\nabla}\cdot$, with respect to curvilinear coordinates $\boldsymbol{\xi}$ that will be used in this paper, it is useful to define the local covariant basis $\boldsymbol{e}_k$ associated to the transformation ϕ given by

$$\boldsymbol{e}_k = \frac{\partial \boldsymbol{x}}{\partial \xi^k} = \frac{\partial x^1}{\partial \xi^k}\,\boldsymbol{i} + \frac{\partial x^2}{\partial \xi^k}\,\boldsymbol{j} + \frac{\partial x^3}{\partial \xi^k}\,\boldsymbol{k}\,,$$

where $k = 1, 2, 3$, and $\boldsymbol{i}$, $\boldsymbol{j}$ and $\boldsymbol{k}$ are vectors of the canonical basis corresponding to the Cartesian coordinates system. The contravariant basis $\boldsymbol{e}^k$ associated to $\boldsymbol{e}_k$ is provided through the relations

$$\boldsymbol{e}^k \cdot \boldsymbol{e}_j = \delta^k_j\,,$$

where δ^k_j is the Krönecker tensor.

With these quantities, the gradient of the vector field $\boldsymbol{V}(\boldsymbol{\xi})$ is given by

$$\boldsymbol{\nabla}\boldsymbol{V} = \frac{\partial \boldsymbol{V}}{\partial \xi^k} \otimes \boldsymbol{e}^k = \left(\frac{\partial \boldsymbol{V}^i}{\partial \xi^k} + \boldsymbol{V}^m \Gamma^i_{mk} \right) \boldsymbol{e}_i \otimes \boldsymbol{e}^k\,.$$

(The Einstein summation convention is assumed through this paper.) Here Γ^i_{mk} are the Christoffel symbols given by

$$\frac{\partial \boldsymbol{e}_m}{\partial \xi^k} = \Gamma^i_{mk} \boldsymbol{e}_i \,,$$

and represent the projection onto $\boldsymbol{e}_i$ of the change of the vector $\boldsymbol{e}_m$ according to ξ^k.
The divergence of the vector field $\boldsymbol{V}(\boldsymbol{\xi})$ is defined as the contraction of the gradient

$$\boldsymbol{\nabla} \cdot \boldsymbol{V} = \frac{\partial \boldsymbol{V}}{\partial \xi^k} \cdot \boldsymbol{e}^k = \left(\frac{\partial \boldsymbol{V}^i}{\partial \xi^k} + \boldsymbol{V}^m \Gamma^i_{mk} \right) \boldsymbol{e}_i \cdot \boldsymbol{e}^k = \frac{\partial \boldsymbol{V}^k}{\partial \xi^k} + \boldsymbol{V}^k \Gamma^i_{ki} \,.$$

By using the identity $\dfrac{1}{J} \dfrac{\partial J}{\partial \xi^k} = \Gamma^i_{ki}$, one gets the compact expression

$$\boldsymbol{\nabla} \cdot \boldsymbol{V} = \frac{1}{J} \frac{\partial (J \boldsymbol{V} \cdot \boldsymbol{e}^k)}{\partial \xi^k} \,.$$

Considering a tensor field $\boldsymbol{T}$, its gradient is given by

$$\boldsymbol{\nabla} \boldsymbol{T} = \frac{\partial \boldsymbol{T}}{\partial \xi^k} \otimes \boldsymbol{e}^k \,.$$

The above relation can be expanded as follows

$$\boldsymbol{\nabla} \boldsymbol{T} = \left(\frac{\partial \boldsymbol{T}^{ij}}{\partial \xi^k} + \boldsymbol{T}^{mj} \Gamma^i_{mk} + \boldsymbol{T}^{im} \Gamma^j_{mk} \right) \boldsymbol{e}_i \otimes \boldsymbol{e}_j \otimes \boldsymbol{e}^k \,. \tag{2.1}$$

The divergence of the tensor field $\boldsymbol{T}$ is given by

$$\boldsymbol{\nabla} \cdot \boldsymbol{T} = \frac{\partial \boldsymbol{T}}{\partial \xi^k} \cdot \boldsymbol{e}^k \,.$$

Using relation (2.1) this leads to

$$\boldsymbol{\nabla} \cdot \boldsymbol{T} = \frac{1}{J} \frac{\partial}{\partial \xi^k} \left(J \boldsymbol{T} \cdot \boldsymbol{e}^k \right) \,.$$

We are now ready to design a finite volume methods in curvilinear coordinates for hyperbolic conservation laws.

3. Contruction of finite volume schemes in curvilinear coordinates

Let us consider a general hyperbolic conservation law equations written in a coordinate free manner as

$$\frac{\partial \boldsymbol{W}}{\partial t} + \boldsymbol{\nabla} \cdot \boldsymbol{F}(\boldsymbol{W}) = 0 \,,$$

where $\boldsymbol{W}$ is the state variable and $\boldsymbol{F}(\boldsymbol{W})$ is its flux.

Let us also consider a curvilinear transformation $\phi : \boldsymbol{\xi} \mapsto \boldsymbol{x}$, whose determinant of Jacobian is J. Using the results of the previous section and noting that $\partial_t J = 0$, it can be seen that in this coordinates system, the above equation becomes

$$\frac{\partial J \boldsymbol{W}}{\partial t} + \frac{\partial}{\partial \xi^k} \left(J \boldsymbol{F}(\boldsymbol{W}) \cdot \boldsymbol{e}^k \right) = 0 \,.$$

In order to see the contour of the problem, we will study separately the construction of finite volume method into two different cases. The first one deals with the scalar case, that is the state variable $\boldsymbol{W}$ is a scalar and its

flux $\boldsymbol{F}(\boldsymbol{W})$ is a vector. In a second step, we will consider the case where $\boldsymbol{W}$ is a vector while its flux $\boldsymbol{F}(\boldsymbol{W})$ is a tensor.

3.1. **Scalar equation**

This corresponds to take $\boldsymbol{W} = S$ a scalar and $\boldsymbol{F}(\boldsymbol{W}) = \boldsymbol{V}$ a vector, then the hyperbolic equation becomes

$$\frac{\partial(J\,S)}{\partial t} + \frac{\partial}{\partial \xi^k}\Big(J\boldsymbol{V}\cdot\boldsymbol{e}^k\Big) = 0\,. \tag{3.2}$$

Typical examples for instance are the equations of continuity and energy in fluid dynamics.

According to the finite volume philosophy, the discrete equations are simply obtained by integrating (3.2) on a control cell. To be more precise, let us consider a subdivision of the computational domain $\Omega(\xi)$ into control volumes $(\Omega_i)_{i\in\mathbb{N}}$. Then integrating equation (3.2) over a cell Ω_i and dividing the result by the volume $|\Omega_i|$, one gets

$$\frac{1}{|\Omega_i|}\int_{\Omega_i}\frac{\partial(J\,S)}{\partial t}\,d\Omega + \frac{1}{|\Omega_i|}\int_{\Omega_i}\frac{\partial}{\partial \xi^k}\Big(J\boldsymbol{V}\cdot\boldsymbol{e}^k\Big)\,d\Omega = 0\,,$$

which can be rewritten as

$$\frac{\partial}{\partial t}\Big(\frac{1}{|\Omega_i|}\int_{\Omega_i} J\,S\,d\Omega\Big) + \frac{1}{|\Omega_i|}\int_{\Omega_i}\frac{\partial}{\partial \xi^k}\Big(J\boldsymbol{V}\cdot\boldsymbol{e}^k\Big)\,d\Omega = 0\,.$$

Introducing the average $S_i = \frac{1}{|\Omega_i|}\int_{\Omega_i} J\,S\,d\Omega$ yields,

$$\frac{\partial}{\partial t}\Big(S_i\Big) + \frac{1}{|\Omega_i|}\int_{\Omega_i}\frac{\partial}{\partial \xi^k}\Big(J\boldsymbol{V}\cdot\boldsymbol{e}^k\Big)\,d\Omega = 0\,.$$

The flux term is also immediately tractable, since by the divergence theorem, one has

$$\int_{\Omega_i}\frac{\partial}{\partial \xi^k}\Big(J\boldsymbol{V}\cdot\boldsymbol{e}^k\Big)\,d\Omega = \int_{\partial\Omega_i} JV_k\big(\boldsymbol{n}\cdot\boldsymbol{e}^k\big)\,d\sigma(\Omega)\,, \tag{3.3}$$

where $\partial\Omega_i$ is the boundary of Ω_i, $\boldsymbol{n}$ is the outward pointing unit vector normal to the surface $\partial\Omega_i$, and $d\sigma(\Omega)$ the Lebesgue measure on this surface. The right hand side of (3.3) is immediately calculable as soon as one has numerical fluxes [3, 5, 9]. For this case, it is readily seen that there is no difference between the construction of finite volume method in curvilinear coordinates system and in a Cartesian one.

3.2. **Vectorial equation**

This case deals with $\boldsymbol{W} = \boldsymbol{V}$ a vector and $\boldsymbol{F}(\boldsymbol{W}) = \boldsymbol{T}$ a tensor, then the hyperbolic equation turns into

$$\frac{\partial(J\,\boldsymbol{V})}{\partial t} + \frac{\partial}{\partial \xi^k}\Big(J\boldsymbol{T}\cdot\boldsymbol{e}^k\Big) = 0\,. \tag{3.4}$$

Momentum equation in fluid dynamics is such a kind of equations.

By using the same procedure as in scalar case, one gets the following discrete scheme,

$$\frac{\partial}{\partial t}\Big(\frac{1}{|\Omega_i|}\int_{\Omega_i} J\,\boldsymbol{V}\,d\Omega\Big) + \frac{1}{|\Omega_i|}\int_{\Omega_i}\frac{\partial}{\partial \xi^k}\Big(J\boldsymbol{T}\cdot\boldsymbol{e}^k\Big)\,d\Omega = 0\,, \tag{3.5}$$

and at first glance, this case seems similar to the scalar one. However, since $\boldsymbol{V}$ is a vector, it has to be stored component by component on a given basis. The traditional approach consists in taking the scalar product of

equation (3.4) by the basis vectors $\boldsymbol{e}^k$ (resp. $\boldsymbol{e}_k$) and then to obtain scalar equations for the covariant components of the vector field $\boldsymbol{V}^k$ (resp. contravariant components $\boldsymbol{V}_k$). Then these scalar equations are discretized using the results of section 3.1. In the sequel, we will designate this method as the projection-integration method. This approach has one important shortcoming: because the basis vectors are spatially dependent, they do not commute with the differential operators and therefore source terms appear in the equations (see equation (4.21) for instance). The approximation of these terms is difficult and moreover it depends on the specific curvilinear system used.
We therefore advocate the use of the following procedure that we will be called the integration-projection method.

First we define an average basis in the cell Ω_i by:

$$\boldsymbol{e}_{i,k} = \frac{1}{|\Omega_i|} \int_{\Omega_i} J\, \boldsymbol{e}_k \, d\Omega \,,$$

so that one obtains, assuming that $V_{i,k}$ is constant in a cell,

$$\frac{1}{|\Omega_i|} \int_{\Omega_i} J\, \boldsymbol{V} \, d\Omega = V_{i,k}\, \boldsymbol{e}_{i,k} \,.$$

Here, $\boldsymbol{e}_{i,k}$ is the kth average vector in the cell Ω_i with respect to the chosen curvilinear coordinates, and by definition $V_{i,k}$ represents the average value of $\boldsymbol{V}$ along the kth vector according to the corresponding curvilinear coordinates. The discrete finite volume approximation is then defined by

$$\frac{\partial}{\partial t} V_{i,k} + \frac{\boldsymbol{e}^{i,k}}{|\Omega_i|} \cdot \int_{\Omega_i} \frac{\partial}{\partial \xi^k} \left(J \boldsymbol{T} \cdot \boldsymbol{e}^k \right) d\Omega = 0 \,, \tag{3.6}$$

where $(\boldsymbol{e}^{i,k})_k$ is the contravariant basis associated to $(\boldsymbol{e}_{i,k})_k$.
This procedure is quite simple and it allows for a general (and implicit) discretisation of the source terms. In the next section we detail it in the case of $2D$ polar coordinates.

4. Application to 2D polar coordinates

The construction of finite volume method proposed in section 3 is illustrated in $2D$ polar coordinates.

4.1. $2D$ polar coordinates and finite volume method

Let us consider $2D$ polar coordinates denoted by $(r,\, \theta) \in (0,\, +\infty[\times[0,\, 2\pi)$ related to Cartesian coordinates $(x,\, y)$ by $(x,\, y) = \phi(r,\, \theta)$ as follows,

$$\left\{ \begin{array}{rcl} x & = & r\, \cos\theta \,, \\ y & = & r\, \sin\theta \,. \end{array} \right.$$

We consider the usual orthonormal basis $(\boldsymbol{e}_x,\, \boldsymbol{e}_y)$ of $\mathbb{R}^2$, and then the covariant basis associated with the coordinates $(r,\, \theta)$ is given by

$$\boldsymbol{e}_r = \left(\begin{array}{c} \cos\theta \\ \sin\theta \end{array} \right) , \quad \boldsymbol{e}_\theta = \left(\begin{array}{c} -r\, \sin\theta \\ r\, \cos\theta \end{array} \right) .$$

The determinant associated to the transformation ϕ is $J = r$ while the contravariant basis with respect to $(\boldsymbol{e}_r,\, \boldsymbol{e}_\theta)$ is given by

$$\boldsymbol{e}^r = \left(\begin{array}{c} \cos\theta \\ \sin\theta \end{array} \right) , \quad \boldsymbol{e}^\theta = \frac{1}{r} \left(\begin{array}{c} -\sin\theta \\ \cos\theta \end{array} \right) .$$

Working with the covariant vector $\boldsymbol{e}_\theta$ and the contravariant vector $\boldsymbol{e}^\theta$ leads to a scale factor r, it is then appropriate to consider their associated unit vectors,

$$\tilde{\boldsymbol{e}_\theta} = \frac{1}{r}\boldsymbol{e}_\theta\,, \quad \tilde{\boldsymbol{e}}^\theta = r\,\boldsymbol{e}^\theta\,.$$

Then, for instance a vector $\boldsymbol{V}$ can be written as $\boldsymbol{V} = V^r\boldsymbol{e}_r + V^\theta\tilde{\boldsymbol{e}_\theta}$.

Equipped with these notations, we can write down the expressions of gradient and divergence operators. The gradient of a scalar function S in polar coordinates writes

$$\boldsymbol{\nabla} S = \partial_r S\,\boldsymbol{e}^r + \frac{1}{r}\partial_\theta S\,\tilde{\boldsymbol{e}^\theta}\,.$$

Let us write the vector $\boldsymbol{V}$ as $\boldsymbol{V} = V^r\boldsymbol{e}_r + V^\theta\tilde{\boldsymbol{e}_\theta}$, its divergence is given by

$$\boldsymbol{\nabla}\cdot\boldsymbol{V} = \frac{1}{r}\partial_r(r\,V^r) + \frac{1}{r}\partial_\theta(r\,V^\theta) = \partial_r V^r + \frac{1}{r}V^r + \partial_\theta V^\theta\,.$$

Now, consider a tensor $\boldsymbol{T}$ decomposed as

$$\boldsymbol{T} = T^{r,r}\,\boldsymbol{e}_r\otimes\boldsymbol{e}_r + T^{r,\theta}\,\boldsymbol{e}_r\otimes\tilde{\boldsymbol{e}_\theta} + T^{\theta,r}\,\tilde{\boldsymbol{e}_\theta}\otimes\boldsymbol{e}_r + T^{\theta,\theta}\,\tilde{\boldsymbol{e}_\theta}\otimes\tilde{\boldsymbol{e}_\theta}\,.$$

The divergence of $\boldsymbol{T}$ is given by the following formula,

$$\begin{aligned}\boldsymbol{\nabla}\cdot\boldsymbol{T} &= \frac{1}{r}\partial_r(r\boldsymbol{T}\cdot\boldsymbol{e}^r) + \frac{1}{r}\partial_\theta(r\boldsymbol{T}\cdot\tilde{\boldsymbol{e}^\theta})\\ &= \frac{1}{r}\partial_r(r\,T^{r,r}\,\boldsymbol{e}_r + r\,T^{r,\theta}\,\tilde{\boldsymbol{e}_\theta}) + \frac{1}{r}\partial_\theta(r\,T^{\theta,r}\,\boldsymbol{e}_r + r\,T^{\theta,\theta}\,\tilde{\boldsymbol{e}_\theta})\,.\end{aligned}$$

Now, let $\boldsymbol{V} = V^r\boldsymbol{e}_r + V^\theta\tilde{\boldsymbol{e}_\theta}$ be a vector which temporal evolution is governed by,

$$\frac{\partial(J\,\boldsymbol{V})}{\partial t} + \frac{\partial}{\partial\xi^k}\left(J\boldsymbol{T}\cdot\boldsymbol{e}^k\right) = 0\,, \tag{4.7}$$

where $\boldsymbol{T}$ is a tensor.

Applying the procedure developed in the previous section, one gets the following scheme,

$$\frac{\partial V_{i,r}}{\partial t}\,\boldsymbol{e}_{i,r} + \frac{\partial V_{i,\theta}}{\partial t}\,\boldsymbol{e}_{i,\theta} + \frac{1}{|\Omega_i|}\int_{\Omega_i}\frac{\partial}{\partial\xi^k}\left(J\boldsymbol{T}\cdot\boldsymbol{e}^k\right)d\Omega = 0\,, \tag{4.8}$$

where $V_{i,r}$ and $V_{i,\theta}$ are average values of V^r and V^θ, respectively in the cell Ω_i, while $\boldsymbol{e}_{i,r}$ and $\boldsymbol{e}_{i,\theta}$ are average vectors in the cell Ω_i,

$$\boldsymbol{e}_{i,r} = \frac{1}{|\Omega_i|}\int_{\Omega_i} r\boldsymbol{e}_r\,d\Omega\,, \quad \boldsymbol{e}_{i,\theta} = \frac{1}{|\Omega_i|}\int_{\Omega_i} r\tilde{\boldsymbol{e}_\theta}\,d\Omega\,.$$

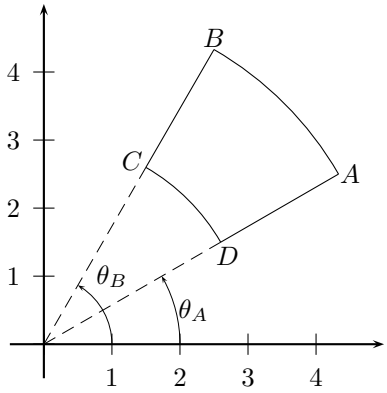

FIG 1: A cell in polar coordinates.

For simplicity, the tensor $\boldsymbol{T}$ is assumed to be symmetric, *i.e.* $T^{r,\theta} = T^{\theta,r}$. We also chose a tensorial mesh so that the cell Ω_i can be localized by the segments product $[r_D,\, r_A] \times [\theta_A,\, \theta_B]$ (see Figure 1). Then the average vectors $\boldsymbol{e}_{i,r}$ and $\boldsymbol{e}_{i,\theta}$ can be expressed as

$$\begin{aligned} \boldsymbol{e}_{i,r} &= \frac{1}{\theta_B - \theta_A}(\boldsymbol{e}_{\tilde{\theta}_A} - \boldsymbol{e}_{\tilde{\theta}_B})\,, \\ \boldsymbol{e}_{i,\theta} &= \frac{1}{\theta_B - \theta_A}(\boldsymbol{e}_{r_B} - \boldsymbol{e}_{r_A})\,, \end{aligned}$$

where

$$\boldsymbol{e}_{r_A} = \boldsymbol{e}_{r_D} = \begin{pmatrix} \cos\theta_A \\ \sin\theta_A \end{pmatrix}, \quad \boldsymbol{e}_{\tilde{\theta}_A} = \boldsymbol{e}_{\tilde{\theta}_D} = \begin{pmatrix} -\sin\theta_A \\ \cos\theta_A \end{pmatrix},$$

and

$$\boldsymbol{e}_{r_B} = \boldsymbol{e}_{r_C} = \begin{pmatrix} \cos\theta_B \\ \sin\theta_B \end{pmatrix}, \quad \boldsymbol{e}_{\tilde{\theta}_B} = \boldsymbol{e}_{\tilde{\theta}_C} = \begin{pmatrix} -\sin\theta_B \\ \cos\theta_B \end{pmatrix}.$$

Finally, for any scalar function $f = f(r, \theta)$, we use the following approximations:

$$\begin{aligned} \hat{f}_{|_{r_D}} \approx f(r_D,\, \theta)\,, \quad \hat{f}_{|_{r_A}} \approx f(r_A,\, \theta)\,, \quad \forall\, \theta \in [\theta_A,\, \theta_B]\,, \\ \hat{f}_{|_{\theta_A}} \approx f(r,\, \theta_A)\,, \quad \hat{f}_{|_{\theta_B}} \approx f(r,\, \theta_B)\,, \quad \forall\, r \in [r_D,\, r_A]\,. \end{aligned}$$

Then equation (4.8) becomes,

$$\begin{aligned} |\Omega_i|\,(\partial_t V_{i,r}\,\boldsymbol{e}_{i,r} + \partial_t V_{i,\theta}\,\boldsymbol{e}_{i,\theta}) + \left(r_A\,\hat{T}^{r,r}_{|_{r_A}} - r_D\,\hat{T}^{r,r}_{|_{r_D}}\right)(\boldsymbol{e}_{\theta_A} - \boldsymbol{e}_{\theta_B}) + \left(r_A\,\hat{T}^{r,\theta}_{|_{r_A}} - r_D\,\hat{T}^{r,\theta}_{|_{r_D}}\right)\left(\boldsymbol{e}_{r_B} - \boldsymbol{e}_{r_A}\right) \\ + (r_D - r_A)\left(\hat{T}^{r,\theta}_{|_{\theta_B}}\,\boldsymbol{e}_{r_B} + \hat{T}^{\theta,\theta}_{|_{\theta_B}}\,\boldsymbol{e}_{\theta_B} - \hat{T}^{r,\theta}_{|_{\theta_A}}\,\boldsymbol{e}_{r_A} - \hat{T}^{\theta,\theta}_{|_{\theta_A}}\,\boldsymbol{e}_{\theta_A}\right) = 0\,. \end{aligned} \tag{4.9}$$

It is interesting to expand equation (4.9) on the pair of orthogonal vectors $\boldsymbol{e}_{i,r}$ and $\boldsymbol{e}_{i,\theta}$, which yields

$$\begin{aligned}|\Omega_i|\,\partial_t V_{i,r} + (\theta_B-\theta_A)\,(r_A\,\hat{T}^{r,r}_{|_{r_A}} - r_D\,\hat{T}^{r,r}_{|_{r_D}}) + \frac{\theta_B-\theta_A}{2}\frac{\sin(\theta_B-\theta_A)}{1-\cos(\theta_B-\theta_A)}(r_A-r_D)\,(\hat{T}^{r,\theta}_{|_{\theta_B}} - \hat{T}^{r,\theta}_{|_{\theta_A}}) \\ - (\theta_B-\theta_A)\,(r_A-r_D)\,\frac{\hat{T}^{\theta,\theta}_{|_{\theta_B}} + \hat{T}^{\theta,\theta}_{|_{\theta_A}}}{2} = 0\,,\end{aligned} \tag{4.10}$$

$$\begin{aligned}|\Omega_i|\,\partial_t V_{i,\theta} + (\theta_B-\theta_A)\,(r_A\,\hat{T}^{r,\theta}_{|_{r_A}} - r_D\,\hat{T}^{r,\theta}_{|_{r_D}}) + \frac{\theta_B-\theta_A}{2}\frac{\sin(\theta_B-\theta_A)}{1-\cos(\theta_B-\theta_A)}(r_A-r_D)\,(\hat{T}^{\theta,\theta}_{|_{\theta_B}} - \hat{T}^{\theta,\theta}_{|_{\theta_A}}) \\ + (\theta_B-\theta_A)\,(r_A-r_D)\,\frac{\hat{T}^{r,\theta}_{|_{\theta_B}} + \hat{T}^{r,\theta}_{|_{\theta_A}}}{2} = 0\,.\end{aligned} \tag{4.11}$$

Equations (4.10)-(4.11) can be considered as results of integration over Ω_i followed by projections onto $\boldsymbol{e}_{i,r}$ and $\boldsymbol{e}_{i,\theta}$ of (4.7). This operation is referred to as integration-projection procedure.
It is convenient to compare equations (4.10)-(4.11) with the result of the traditional approach, that is projection-integration procedure applied to (4.7). The projection of (4.7) onto $\boldsymbol{e}_r$ and $\boldsymbol{e}_\theta$ leads to,

$$\partial_t(r\,V_r) + \partial_r(r\,T^{r,r}) + \partial_\theta T^{r,\theta} = T^{\theta,\theta}\,, \tag{4.12}$$

and

$$\partial_t(r\,V_\theta) + \partial_r(r\,T^{r,\theta}) + \partial_\theta T^{\theta,\theta} = -T^{r,\theta}\,. \tag{4.13}$$

Equations (4.12)-(4.13) are no longer conservative since they own right hand side source terms, the conservative character of the original equation (4.7) is lost during the projection operation. This is due to variations of vectors $\boldsymbol{e}_r$ and $\boldsymbol{e}_\theta$ with respect to θ. This kind of source terms does not appear if Cartesian coordinates are considered in lieu of polar coordinates.
Now, integrating (4.12)-(4.13) yield,

$$|\Omega_i|\,\partial_t V_{i,r} + (\theta_B-\theta_A)\,(r_A\,\hat{T}^{r,r}_{|_{r_A}} - r_D\,\hat{T}^{r,r}_{|_{r_D}}) + (r_A-r_D)\,(\hat{T}^{r,\theta}_{|_{\theta_B}} - \hat{T}^{r,\theta}_{|_{\theta_A}}) = \int_{\Omega_i} T^{\theta,\theta}(r,\theta)\,dr\,d\theta\,, \tag{4.14}$$

$$|\Omega_i|\,\partial_t V_{i,\theta} + (\theta_B-\theta_A)\,(r_A\,\hat{T}^{r,\theta}_{|_{r_A}} - r_D\,\hat{T}^{r,\theta}_{|_{r_D}}) + (r_A-r_D)\,(\hat{T}^{\theta,\theta}_{|_{\theta_B}} - \hat{T}^{\theta,\theta}_{|_{\theta_A}}) = -\int_{\Omega_i} T^{r,\theta}(r,\theta)\,dr\,d\theta\,. \tag{4.15}$$

The comparison of equation (4.10) with (4.14), and (4.11) with (4.15) is summarized in the following result.

Proposition 1. *The integration-projection procedure and projection-integration operation applied to vectorial equation written in 2D polar coordinates are equivalent if and only if the source terms are discretized as follows*

$$\begin{aligned}\int_{\Omega_i} T^{\theta,\theta}(r,\theta)\,dr\,d\theta &= (\theta_B-\theta_A)\,(r_A-r_D)\,\frac{\hat{T}^{\theta,\theta}_{|_{\theta_B}} + \hat{T}^{\theta,\theta}_{|_{\theta_A}}}{2} \\ &+ \left(1 - \frac{\theta_B-\theta_A}{2}\frac{\sin(\theta_B-\theta_A)}{1-\cos(\theta_B-\theta_A)}\right)(r_A-r_D)\,(\hat{T}^{r,\theta}_{|_{\theta_B}} - \hat{T}^{r,\theta}_{|_{\theta_A}})\,,\end{aligned} \tag{4.16}$$

$$\begin{aligned}\int_{\Omega_i} T^{r,\theta}(r,\theta)\,dr\,d\theta &= (\theta_B-\theta_A)\,(r_A-r_D)\,\frac{\hat{T}^{r,\theta}_{|_{\theta_B}} + \hat{T}^{r,\theta}_{|_{\theta_A}}}{2} \\ &- \left(1 - \frac{\theta_B-\theta_A}{2}\frac{\sin(\theta_B-\theta_A)}{1-\cos(\theta_B-\theta_A)}\right)(r_A-r_D)\,(\hat{T}^{\theta,\theta}_{|_{\theta_B}} - \hat{T}^{\theta,\theta}_{|_{\theta_A}})\,.\end{aligned}$$

Moreover, this discretisation is consistent both on r and θ.

Note that the discrete version of each source term can be split into a centered ("traditional") term and a viscous-like term. The expression of this viscous term is new to the best of our knowledge. Note specially that it couples the components of the tensor $\boldsymbol{T}$.

4.2. **Tools for practical implementation**

In this section we gather together tools that are important for pratical implementation of a part or of the full model system composed of a continuity and momentum equations

$$\begin{cases} \partial_t n + \boldsymbol{\nabla}.(n\boldsymbol{V}) = 0\,, \\ \partial_t(n\boldsymbol{V}) + \boldsymbol{\nabla}.(n\boldsymbol{V}\otimes\boldsymbol{V} + n\boldsymbol{I}) = 0\,. \end{cases} \tag{4.17}$$

Here, n is the density per unit mass, $\boldsymbol{V}$ is the velocity and $\boldsymbol{I}$ the unit tensor. Both the Cartesian version of system (4.17) and its counterpart in $2D$ polar coordinates are investigated, and the results obtained by both methods are compared.

The cells of the mesh used in Cartesian coordinates are quadrilaterals while they are curved ones in $2D$ polar coordinates system. In the two cases, we use the same nodes to construct the mesh, but we emphasize that the cells are different from one coordinates system to another. In Figure 2 are displayed two such kinds of meshes where the number of radial cells $N_r = 3$ while those of azimuthal ones is $N_\theta = 6$. The radial and azimuthal mesh steps are denoted by Δr and $\Delta\theta$ accordingly, so that for a uniform mesh in azimuthal direction, one has $\Delta\theta = \frac{2\pi}{N_\theta}$.

FIG 2: Cartesian and polar meshes.

In finite volume method implementation, we need to know the value of areas of mesh cells. Consider a generic cell Ω_i in $2D$ polar coordinates localized by its four nodes A, B, C, and D as in Figure 1, the measure of this area is given by,

$$|\Omega_i|_{r,\theta} = \left(r + \frac{\Delta r}{2}\right)\,\Delta r\,\Delta\theta\,. \tag{4.18}$$

If these nodes are used to construct a cell Ω_i in a Cartesian coordinates, the measure of the area of this cell will be

$$|\Omega_i|_{x,y} = \left(r + \frac{\Delta r}{2}\right)\,\Delta r\,\sin\Delta\theta\,. \tag{4.19}$$

Now, by taking $\Delta\theta$ small *i.e.* $\Delta\theta \to 0$ in equation (4.19), one gets

$$|\Omega_i|_{r,\theta} \approx |\Omega_i|_{x,y}\,,$$

which makes obvious the fact that for large N_θ, meshes obtained in Cartesian and $2D$ polar coordinates systems are approximately equal.

Next, we are interested in evaluating the integral of normal vectors along edges of mesh cells. The tricky one seems to be those corresponding to curved edges as shown in Figure 3. Thanks to the divergence theorem,

$$\oint \boldsymbol{n}\, dl = 0\,,$$

we deduce

$$\int_{\widehat{AB}} \boldsymbol{n}\, dl = \int_{\overline{AB}} \boldsymbol{n}\, dl\,,$$

which can be immediately calculated by knowning only the coordinates of the nodes A and B.

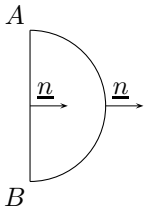

FIG 3: Normals.

We are now concerned with the construction of numerical fluxes for hyperbolic equations written in general curvilinear coordinates in 2D. Assume we have in our hand a numerical flux procedure, consult [3,5,9] for more details. The following is a possible algorithm that allows us to construct a numerical flux in general curvilinear coordinates of cells Ω_i and Ω_j:

- Write the vectorial quantities of cells Ω_i and Ω_j according to the orthogonal basis $(\boldsymbol{n}_{ij}, \boldsymbol{\tau}_{ij})$ of the intercell boundary $\partial\Omega_{ij}$ between the cells Ω_i and Ω_j, ($\boldsymbol{n}_{ij}$ being the outward pointing unit vector normal to the $\partial\Omega_{ij}$ directed from the cell Ω_i to the cell Ω_j, $\boldsymbol{\tau}_{ij}$ is an unit vector orthogonal to $\boldsymbol{n}_{ij}$). Let $\overline{\Omega_i}$ and $\overline{\Omega_j}$ be the results of this step;
- Compute the flux $\boldsymbol{\Phi}_{ij}$ with the states $\overline{\Omega_i}$ and $\overline{\Omega_j}$ with respect to the intercell boundary $\partial\Omega_{ij}$ by using a chosen numerical flux [3,5,9];
- Project the flux $\boldsymbol{\Phi}_{ij}$ onto the cells Ω_i and Ω_j to get fluxes $\boldsymbol{\Phi}_i$ and $\boldsymbol{\Phi}_j$ respectively, according to

$$\begin{aligned}\boldsymbol{\Phi}_i &= (\boldsymbol{\Phi}_{ij}\cdot\boldsymbol{e}_{i,r})\,\boldsymbol{e}_{i,r} + (\boldsymbol{\Phi}_{ij}\cdot\boldsymbol{e}_{i,\theta})\,\boldsymbol{e}_{i,\theta}\,,\\ \boldsymbol{\Phi}_j &= (\boldsymbol{\Phi}_{ij}\cdot\boldsymbol{e}_{j,r})\,\boldsymbol{e}_{j,r} + (\boldsymbol{\Phi}_{ij}\cdot\boldsymbol{e}_{j,\theta})\,\boldsymbol{e}_{j,\theta}\,,\end{aligned}$$

  where $(\boldsymbol{e}_{i,r}, \boldsymbol{e}_{i,\theta})$ is the average vector basis in the cell Ω_i, $(\boldsymbol{e}_{j,r}, \boldsymbol{e}_{j,\theta})$ is those of the cell Ω_j.

We turn now to numerical tests in $2D$ polar coordinates in order to validate our approach.

4.3. **Advection equation test**

The first test concerns a scalar advection equation with a constant azimuthal velocity,

$$\partial_t n + \boldsymbol{\nabla}.(n\boldsymbol{V}) = 0\,,$$

which in polar coordinates takes the form,

$$\partial_t rn + \partial_r(rnV_r) + \partial_\theta(nV_\theta) = 0\,.$$

We consider the following initial conditions (Fig. 4): $\forall (r,\theta) \in \Omega$:

- for the density: $n(r,\theta) = n_0\,,$
- for the velocity: $V_r(r,\,\theta) = 0$ and $V_\theta(r,\,\theta) = V_0,$

where n_0 and V_0 are constants. For our test, $n_0 = 1$ and $V_0 = 0.5$.

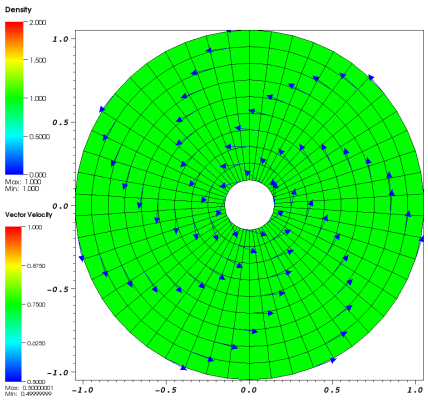

FIG 4: IC with Cartesian mesh.

For the boundary conditions we set a null flux.

In this case, we obtain similar results with Cartesian and polar methods: the solutions are preserved as expected. The error in both cases is in the order of machine epsilon. Note that for scalar equation, only the cell areas are different but the flux is the same whence the similar results.

4.4. **Isothermal Euler system**

The following tests concern the isothermal Euler system. Here, we consider a scalar and a vectorial equations. As consequence, as well as the areas, the computation of the fluxes is different.

More precisely, we are interested in the following dimensionless system where the temperature is supposed constant,

$$\left\{\begin{array}{r} \partial_t n + \boldsymbol{\nabla}.(n\boldsymbol{V}) = 0\,, \\ \partial_t(n\boldsymbol{V}) + \nabla.(n\boldsymbol{V}\otimes\boldsymbol{V}) + \boldsymbol{\nabla} n = 0\,. \end{array}\right. \tag{4.20}$$

We use this system for two test cases. The first one considers a constant density and an azimuthal velocity. With the second one, the Gresho test, we can compare the two methods on a stationary solution.

4.4.1. *Constant density and velocity*

The initial conditions in this test are a constant density and an azimuthal velocity:

- for the density: $n(r,\theta) = n_0,\ \forall\,(r,\theta) \in \Omega,$
- for the velocity: $V_r(r,\theta) = 0$ and $V_\theta(r,\theta) = V_0,\ \forall\,(r,\theta) \in \Omega,$

where n_0 and V_0 are constants, typically $n_0 = 1$ and $V_0 = 0.5$ for our test.

For the boundary conditions we impose slippery walls.

Figures 5 represent the Cartesian and polar results.

Note here that a radial velocity appears and comes from the source term. Indeed, if we consider the isothermal Euler system in polar coordinates, we obtain:

$$\left\{\begin{array}{r} \partial_t n + \partial_r(rnV_r) + \partial_\theta(nV_\theta) = 0\,, \\ \partial_t rV_r + \partial_r(r(nV_r^2 + n)) + \partial_\theta nV_rV_\theta = nV_\theta^2 + n\,, \\ \partial_t rV_\theta + \partial_r r(nV_\theta V_r) + \partial_\theta(nV_\theta^2 + n) = -nV_rV_\theta\,. \end{array}\right. \tag{4.21}$$

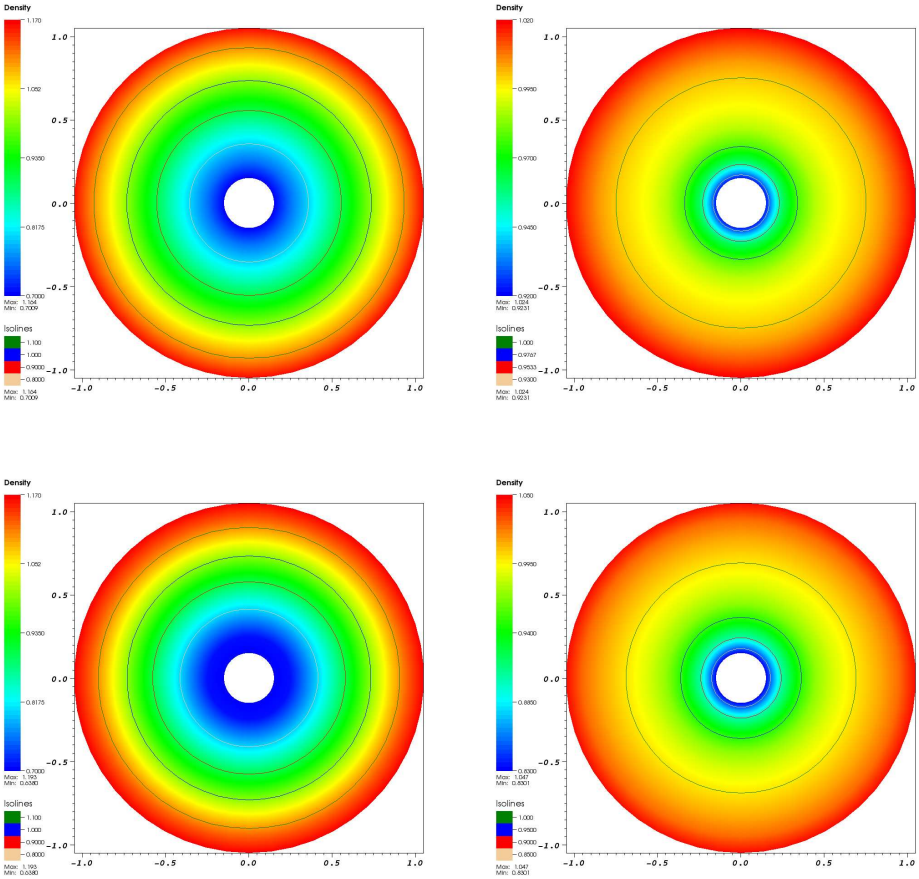

FIG 5: Cartesian results for density at $t = 0.83, 1.69$ on first line; polar results for density at $t = 0.82, 1.65$ on second line.

With the initial conditions, the second equation of the system (4.21) becomes,

$$\partial_t r V_r = n V_\theta^2 .$$

As consequence, a centripetal force appears and then a radial velocity is created.
We note that the numerical results (Fig. 5) match those of physical problems in which a radial velocity appears and then a new profile of the density is obtained. Nevertheless, even if the Cartesian and the polar methods present similar results, it is difficult to compare the two approaches in absence of a stationary solution.

4.4.2. *Gresho test*

The aim of this last test is to compare explicitly the polar and the Cartesian methods with a stationary solution.

To have a stationary solution, first, we suppose,

$$V_r = 0 \quad \text{and} \quad \partial_\theta = 0 .$$

With these assumptions, system (4.21) becomes,

$$\begin{cases} \partial_t n = 0\,, \\ \partial_t r V_r + r\partial_r n = n V_\theta^2\,, \\ \partial_t V_\theta = 0\,. \end{cases} \tag{4.22}$$

We have a stationary solution if the velocity and the density satisfy,

$$r\partial_r n = n V_\theta^2\,. \tag{4.23}$$

For example, if we choose the velocity as a constant,

$$V_\theta = 1\,,$$

with equation (4.23), we obtain the following density profile,

$$n(r) = n(1) r\,.$$

For the boundary conditions we choose influx and outflux computed from the density and the velocity analytic profiles.

Figure 6 shows density profiles for stationary solution (black) and polar and Cartesian methods (respectively, blue and red) with a small $N_\theta = 4$, where $n(1) = 2$ is chosen. Note that even if the mesh is not refined in θ, the polar method gives a solution close to the stationary one whereas the Cartesian method solution is completely different. As consequence, in this case, when N_θ is small, the polar method is better than the Cartesian one.

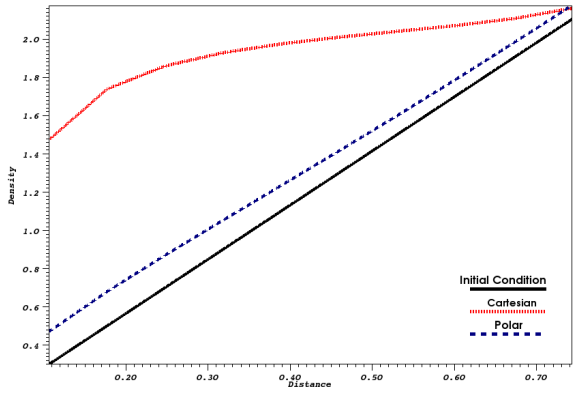

FIG 6: Density profiles for stationary, polar and Cartesian solutions.

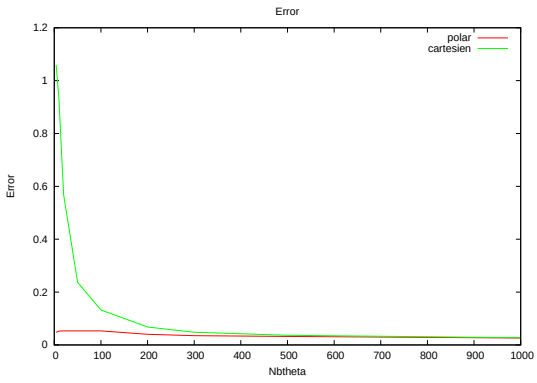

FIG 7: Polar and Cartesian L^2-errors density.

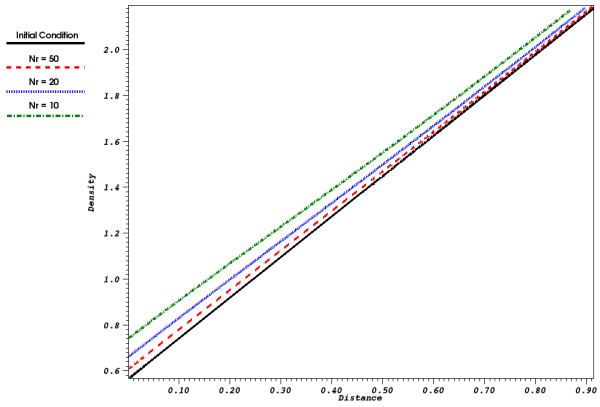

FIG 8: Density profiles for polar solutions in the cases : stationary and $Nr = 10, 20, 50$ with $N_\theta = 4$.

Figure 7 shows the L^2-error for the density computed with polar and Cartesian methods, which confirms the superiority of the polar scheme over the Cartesian one. Errors remain small when the polar method is used for small N_θ. Nevertheless, as we already noted in the previous part, when N_θ becomes large, the polar and Cartesian methods tend to be equivalent, as it should be. In addition, we note that whatever the N_θ chosen, the L^2-error is the same in polar method. Indeed, the error depends only on the chosen N_r (Fig. 8).

5. Conclusion

In this paper, finite volume methods in general curvilinear coordinates for hyperbolic conservation laws have been investigated. This approach has been applied to realistic problems coming from fluid dynamics in tokamak geometry, precisely in $2D$ polar coordinates. Comparison with finite volume in Cartesian coordinates system has confirmed the advantage to use our approach.

Fourthcoming works will consist in extending our approach to toroidal geometry, and to unstructured meshes, and to apply the obtained schemes to physical problems of fusion in tokamaks, for instance ELM instabilities and edge turbulence plasmas simulations.

References

[1] M.A. Beer, S.C. Cowley, G.W. Hammett, Field-aligned coordinates for nonlinear simulations of tokamak turbulence, *Physics of Plasma* **2**, 2687 (1995).
[2] A.M. Dimits, Fluid simulations of tokamak turbulence in quasiballooning coordinates, *Physical Reviews E* **48**, 4070 (1993).
[3] H. Guillard, R. Abgrall, *Modélisation Numérique des Fluides Compressibles*, Series in Applied Mathematics, **5**, Gauthier-Villars, Paris, North-Holland, Amsterdam (2001).
[4] J.P. Goedbloed, S. Poedt, *Principles of Magnetohydrodynamics: With Applications to Laboratory and Astrophysical Plasmas*, Cambridge University Press, Cambridge (2004).
[5] E. Godlewski, P.-A. Raviart, *Numerical Approximation of Hyperbolic System of Conservation Laws*, Applied Mathematics Sciences, **118**, Springer, New York (1996).
[6] R.D. Hazeltine, J.D. Meiss, *Plasma Confinement*, Dover publications INC, Mineola, New York (2003).
[7] J. Pedlosky, *Geophysical Fluid Dynamics*, 2*nd* Edition, Springer, New York (1987).
[8] B.B. Kadomtsev, *Tokamak plasma, a complex physical system*, Institute of Physics Publishing, Bristol (1993).
[9] E.F. Toro, *Riemann Solvers and Numerical Methods in Fluid Dynamics, A Practical Introduction*, 3*rd* Edition, Springer, Heidelberg (2009).
[10] J. Wesson, *Tokamaks*, third edition, International Series of Monographs on Physics, **118**, Oxford Sciences Publications, Oxford (2004).